

## Research on Unequal Error Protection with Punctured Turbo Codes in JPEG Image Transmission System

A. Moulay Lakhdar<sup>1</sup>, R. Méliani<sup>2</sup>, M. Kandouci<sup>2</sup>

**Abstract:** An investigation of Unequal Error Protection (UEP) methods applied to JPEG image transmission using turbo codes is presented. The JPEG image is partitioned into two groups, i.e., DC components and AC components according to their respective sensitivity to channel noise.

The highly sensitive DC components are better protected with a lower coding rate, while the less sensitive AC components use a higher coding rate. While we use the s-random interleaver and s-random odd-even interleaver combined with odd-even puncturing, we can fix easily the local rate of turbo-code. We propose to modify the design of s-random interleaver to fix the number of parity bits. A new UEP scheme for the Soft Output Viterbi Algorithm (SOVA) is also proposed to improve the performances in terms of Bit Error Rate (BER) and Peak Signal to Noise Ratio (PSNR). Simulation results are given to demonstrate how the UEP schemes outperforms the equal error protection (EEP) scheme in terms of BER and PSNR.

**Keywords:** JPEG, Turbo-code, puncturing, BER (Bit Error Rate), Unequal Error Protection (UEP), Peak Signal to Noise Ratio (PSNR).

### 1 Introduction

Visual signals such as compressed still images are very vulnerable to channel noise. Usually, channel coding is utilized to protect the transmitted visual signals. The Joint Photograph Experts Group (JPEG) standard [1] proposed in 1992 is widely used for still image compression and transmission. Turbo codes [2] are suitable for protecting multimedia signals such as images since these visual signals are characterised by a large amount of data, even after compression. In this paper, we address the special case of JPEG still image transmission over noisy channels in which turbo codes are used for channel coding. UEP, which involves data partition with different coding rates, is a

---

<sup>1</sup>Département de Génie Mécanique, Centre Universitaire de Béchar, Béchar 08000, Algérie  
E-mail: Moulaylakhdar78@yahoo.fr

<sup>2</sup>Département d'Electronique Faculté des Sciences de l'Ingénieur, Université Djillali Liabès BP 89, SIDI BEL ABBES, ALGERIE

method used to protect different components of an image “unequally” according to their respective sensitivity to channel errors.

In a JPEG coded image, the coded bits are composed mainly of two types of bits, DC bits and AC bits. There are two justifications in applying UEP to JPEG coded images. First, in the two dimension discrete cosine transform (DCT) adopted by JPEG coding, the DC coefficient is a measure of the average value of the 64 image samples and contains a significant fraction of total image energy. Thus, the DC coefficients are treated separately from the AC coefficients in various source coding stages of JPEG. Secondly, due to strong correlation in adjacent DC bits, differential coding is applied to DC components. Thus, for DC bits, decoding errors in one block will lead to decoding errors in subsequent blocks. Conversely, for AC bits, decoding errors only affect local blocks.

Observing the output bits from a JPEG image encoder, we found AC bit number is around 6-12 times that of DC.

This gives us a large space for applying UEP turbo coding on the output bits of a JPEG source encoder. We allocate a lower coding rate to highly sensitive DC components and a higher coding rate to less sensitive AC components, while keeping the UEP coding rate the same as that of EEP. In order to improve the performances of the turbo codes in term of the BER, we propose a UEP method adapted to the SOVA algorithm. This method is based on high error protection at the beginning of decoding trellis. We will show how sensitive the BER and PSNR of an image is to different protection levels for DC, AC components and the beginning of decoding trellis. In this case the average BER of the AC component is lower than that of EEP, who is not obtained in [7]. Ideal synchronization is assumed in the simulation results.

This paper is organized as follows: in Section 2, we briefly present the system used in our simulations for the transmission of turbo-coded compressed image over Gaussian channels. Then, in Section 3, we present different UEP techniques used in our simulation. Finally, in Section 4, results obtained by our techniques are compared to those obtained with the classical EEP technique.

## **2 The Image Transmission System Used For Simulations**

Fig. 1 represents the image transmission system for which we evaluate the TEB and PSNR after decoding. An input image is compressed by JPEG. The binary symbols resulting from the JPEG compressing constitute the sequence of data to be transmitted. The coder of channel receiving these data is a standard turbo-coder of rate 1/3 [4]. He is obtained by parallel concatenation of two Recursive systematic convolutional codes (RSC), of rate 1/2, constraint length  $K = 5$ , and codes 35/23 in octal notation, separated by an interleaver (Fig. 2). The code RSC, which has these codes, is powerful in term of the free distance.

The JPEG source encoder used in this study partitions the output bits into two groups of bits, i.e., DC bits and AC bits. Both are sent into a multi-rate turbo encoder. The multi-rate turbo encoder applies different coding rates to the DC and AC bits according to the particular UEP scheme. We assume that the channel is a binary input channel with Additive White Gaussian Noise (AWGN). QPSK modulation is used. The turbo decoder decodes the UEP coded bits from the noisy channel output. The JPEG image decoder integrates the two groups of DC and AC bits into a standard image coded stream and outputs the reconstructed image.

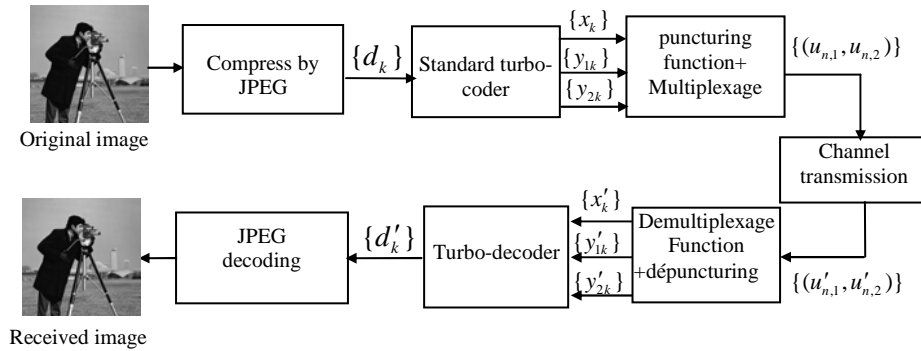


Fig. 1 – A block diagram of a communication system.

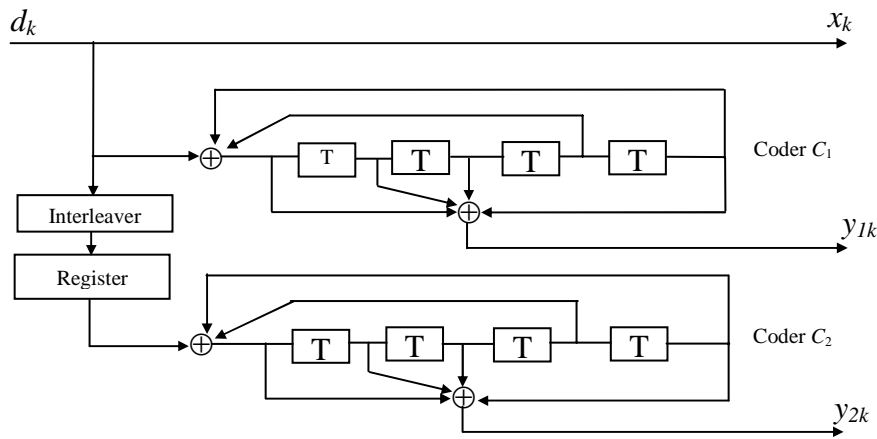


Fig. 2 – Standard turbo-coder structure.

## 2.1 The puncturing

If we use the puncturing [8] technique, it is possible to provide turbo-coders of various rates, starting from only standard code of rate 1/3. The codes obtained present performances very close to those obtained with optimal codes

(unpunctured) of the same rate, in condition that the puncturing matrix is quite selected. This puncturing technique makes it possible to simplify the trellis since in each state converges, only, two branches and not  $2^M$  branches as for an optimal code of rate  $M/N$ . This decreases the complexity of decoding using the Soft Output Viterbi Algorithm (SOVA). Moreover, the same turbo-decoder can be used for any compatible punctured code.

A puncturing matrix  $P$  of period  $p$  applied to a turbo code having  $N$  output branches can be represented by:

$$P = \begin{bmatrix} g_{11} & \cdots & g_{1p} \\ \vdots & g_{ik} & \vdots \\ g_{N1} & \cdots & g_{Np} \end{bmatrix}, \quad (1)$$

where every row corresponds to one output branch, i.e. the first row corresponds to the systematic branch  $\{d_k\}$  (Fig. 2); the second row corresponds to the first parity branch  $\{y_{1k}\}$  and so on. Note that  $g_{ik} \in \{0,1\}$  where 0 implies that corresponding bit is punctured. The degree of freedom in controlling the code rate can be gained by increasing  $p$ . Note that in our case  $N = 3$ .

If  $w(\cdot)$  is the Hamming weight operator, then the rate of the code after puncturing with the puncturing matrix  $P$  is:

$$R = p / w(P). \quad (2)$$

For the unpunctured case:

$$w(P) = Np, \quad (3)$$

and (2) reduces to:

$$R = 1 / N. \quad (4)$$

A simple method consists to puncture only the parity bits, therefore it is necessary to choose a puncturing matrix which coefficients associated with the sequence of information bits  $\{d_k\}$  (Fig. 2) are always equal to 1. Such a matrix is known as “*invariant*” and this puncturing technique is called “puncturing of the parity data”, noted PPD will be adopted during the simulation of the image transmission system described previously. The matrix of puncturing odd-even (EEP) used in our simulation to obtain a code of rate 1/2 is as follows:

$$P = \begin{bmatrix} 1 & 1 \\ 0 & 1 \\ 1 & 0 \end{bmatrix}, \quad (5)$$

with  $p = 2$ . Several work showed the improvement of the performances in these turbo-codes by using an interleaver having the property odd-even.

## 2.2 The interleaving

There are two families of interleavers: block interleaving and convolutionnel interleaving. For example, the family of block interleaving gathers several types of interleaving like the classical interleaver (uniform), pseudo-random (Berrou-Glavieux), random... etc. We are mainly interested in block interleaving [5].

The random interleaver is generated using a purely random vector [6]. The S-random interleaver is a random interleaver with a restriction of his dispersion capacity [5, 6]. For the turbo-code of rate  $R = 1/2$  (punctured), the odd-even interleaver makes an improvement of the performances [6]. He is generated with the following condition: the bits having odd positions (respectively even) are permuted to odd positions (respectively even).

## 3 UEP Schemes

The multi-rate turbo encoder used for UEP [9] is capable of implementing two different code rates for the DC and AC components. Two different structures were examined. We denote DC bit number and AC bit number in a JPEG image by LDC and LAC respectively. In the first structure, the DC and AC blocks are joined together to form a single block of the same size as that of the EEP scheme. The overall block has its same interleaver. Fig. 3 shows the first structure type. The second structure design is to break the larger stream of size  $LDC + LAC$  into  $x$  smaller pieces, each having an identical size of  $y$  bits.  $y$  is the trellis depth of SOVA decoder.

We have

$$x = \left\lceil \frac{L_{DC}}{l_{DC}} \right\rceil, \quad (6)$$

where  $l_{DC}$  is a DC bits number in each piece.

Each piece contains  $l_{DC}$  DC bits and “ $l_{AC} = y - l_{DC}$ ” AC bits. This  $x$  smaller pieces is followed by “ $L_{DC} + L_{AC} - yx$ ” AC remained bits.

The structure is showed in Fig. 4. Using the same inteleaver size for EEP and UEP simplifies the turbo encoder which is desirable from the point of view of hardware implementation. Through varying the number of coded bits associated with each information bit, a multi-rate turbo encoder is obtained.

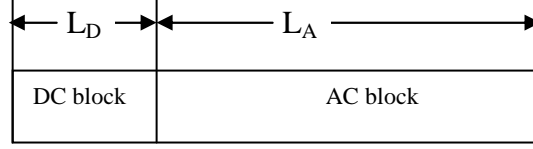


Fig. 3 – The first structure type.

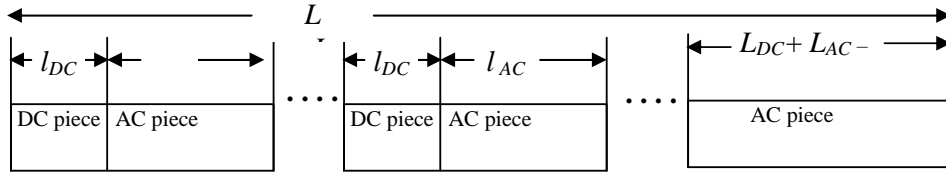


Fig. 4 – The second structure type.

### 3.1 First puncturing matrix

The puncturing matrix for the first structure has a period  $p = L_{DC} + L_{AC}$  and  $N = 3$  represented by:

$$P = \begin{bmatrix} g_{11} \cdots g_{1L_{DC}} \cdots g_{1p} \\ g_{21} \cdots g_{2L_{DC}} \cdots g_{2p} \\ g_{31} \cdots g_{3L_{DC}} \cdots g_{3p} \end{bmatrix}, \quad (7)$$

$$P_1 = g_{11} \cdots g_{1L_{DC}} \cdots g_{1p} = [1111111 \cdots 1111], \quad (8)$$

$$P_3 = g_{31} \cdots g_{3L_{DC}} \cdots g_{3p} = [010101 \cdots 0101], \quad (9)$$

$$P_2^{DC} = g_{21} \cdots g_{2L_{DC}}, \quad (10)$$

$$P_2^{AC} = g_{2L_{DC}+1} \cdots g_{2p}. \quad (11)$$

And the first parity branch ( $P_2$ ) depend on the local rate of DC bits and AC bits: RDC and RAC respectively. For example

$$P_2^{DC} = [1 \ 1 \ 1 \ 1 \ 1 \ 0 \ \cdots 111110], \quad (12)$$

$$P_2^{AC} = [\underbrace{00101010 \ \cdots 10101000}_{48 \text{ bits}} \cdots \underbrace{00101010 \ \cdots 10101000}_{48 \text{ bits}}], \quad (13)$$

for  $R_{DC} = 0.4285$  and  $R_{AC} = 0.5055$ .

We will use tow type of interleavers:

- a) In the case of **S-random odd-even** interleaver: The number of coded bits associated with DC information bit is:  $L_{DC} / 2$  for the second parity branch. Because only the even positions information bits are interleaved towards even positions. And these positions have no null bits of parity.
- b) In the case of **S-random** interleaver: we added in the design of interleaver the following constraint:
- c) The half number of DC bits ( $L_{DC} / 2$ ) must interleaved towards even positions. These  $L_{DC} / 2$  bits are selected randomly. Thus the number of coded bits associated with DC information bit is:  $L_{DC} / 2$  for the second parity branch.

So in the tow case RDC and RAC depend on the first parity branch:  $w(P_2^{DC})$  and  $w(P_2^{AC})$  respectively. We have:

$$w(P_3) = \frac{L_{DC} + L_{AC}}{2}, \quad (14)$$

then the local rate

$$R_{DC} = \frac{L_{DC}}{\left( L_{DC} + w(P_2^{DC}) + \frac{L_{DC}}{2} \right)}, \quad (15)$$

and

$$R_{AC} = \frac{L_{AC}}{\left( L_{AC} + w(P_2^{AC}) + \frac{L_{AC}}{2} \right)}. \quad (16)$$

### 3.2 Second puncturing matrix

The puncturing matrix for the first structure has a period  $p = y$  and  $N = 3$  represented by:

$$P' = \begin{bmatrix} g_{11} \cdots g_{1L_{DC}} \cdots g_{1p} \\ g_{21} \cdots g_{2L_{DC}} \cdots g_{2p} \\ g_{31} \cdots g_{3L_{DC}} \cdots g_{3p} \end{bmatrix}. \quad (17)$$

The same reasoning and interleavers design are applied for this scheme. For  $R_{DC} = 0.4$  and  $R_{AC} = 0.5086$ , we have:

$$P_2'^{DC} = g_{21} \cdots g_{2L_{DC}} = [111 \cdots 11], \quad (18)$$

$$P_2'^{AC} = g_{2l_{DC}+1} \cdots g_{2l_{AC}} = [101010101000 \cdots 101010101000]. \quad (19)$$

This puncturing matrix protect the first  $l_{DC}$  information bits with a low local rate, so in the SOVA decoding we will minimise the probability of choosing the bad way in the beginning of trellis. Then the BER will be minimum with improving the performances of UEP turbo codes.

#### 4 Simulation Results

In this section, we present some simulation results from transmitting JPEG coded “Lena” over the AWGN channel. In JPEG image source coding, quality factor Q is used to control the compression ratio and thus the compressed image quality. A 16 state multi-rate systematic turbo codec with codes 35/23 in octal notation is used in the simulations. S-random and S-random odd-even interleaving is used. The PSNR of “Lena” 64 x 64 image are 34.64. He is the highest PNSR the receiver can obtain without any transmission errors. Synchronisation is an issue when variable length coded (VLC) signals such as JPEG images are transmitted through noisy channels. In order to distinguish synchronisation errors from decoding errors, we assume ideal synchronisation within the DCT operational 8x8 subblock in our simulations. In [3], the authors investigated the UEP method applied to header bits and all the other image bits. In this study, we assume all the header bits are transmitted correctly. And in [7], the authors investigated the UEP method witch interleaver structure design is to break the larger interleaver of size  $L_{AC} + L_{DC}$  into smaller pieces without changing the order of the image bit stream before coding by the turbo coder, each having an identical size of bits, and the interleaving is applied separately to DC bits then to AC bits. In this study, the interleaving is applied once to all the bits of image ( $L_{AC} + L_{DC}$ ).

UEP schemes using the first structure were simulated for the 64×64 “Lena” image.  $L_{DC}$  is 728 and  $L_{AC}$  is 11182. Tow different coding rate allocations for DC and AC components were tried while keeping the total turbo coded bits the same as in the EEP case, i.e., overall rate 1/2 coding regardless of the code rate allocation between the DC and AC components. Figs. 5 and 6 give PSNR performances comparisons for tow different interleavers: S-random and S-random odd-even while Figs. 7 and 8 give BER performance comparisons.

An UEP scheme using the second structure was also simulated for the 64×64 “Lena” image.  $L_{DC}$  is 728 and  $L_{AC}$  is 11182.  $x$ ,  $y$  and  $l_{DC}$  are 104, 95 and 7, respectively. Figs. 9 and 10 give PSNRs performances comparisons while Figs. 11 and 12 give BER performance comparisons. In this case, the average

PSNRs of UEP outperform that of EEP in all interesting  $E_b/N_0$  regions for the  $S$ -random interleaver.

For the first structure type, the PSNRs performances of the UEP schemes are worse than that of the EEP scheme for high  $E_b/N_0$ . The underlying justification is that the error protection is condensed at the beginning of the image bit stream in the DC components. Conversely, for the second structure type, the error protection is distributed over the image bit stream. And the UEP scheme is adapted to the SOVA algorithm (Section 3.2).

Moreover if the two structures are compared in terms of BER (Figs. 7, 8, 11 and 12), we see that the UEP BER and AC BER for the first structure are superior that EEP BER, but it is the reverse in the second structure for the  $S$ -random interleaver.

For the second structure, the average PSNRs of UEP outperform that of EEP for low  $E_b/N_0$ , but is worse than that of EEP for high  $E_b/N_0$  for the  $S$ -random odd-even interleaver and better for the  $S$ -random interleaver for high  $E_b/N_0$ . The underlying justification is that the  $S$ -random odd-even interleaver is very adapted with the odd-even puncturing (EEP) according to their definition. This is obvious on the diagrams of BER in Figs. 11 and 12: UEP BER is superior than EEP BER for high  $E_b/N_0$  especially for  $S$ -random odd-even interleaver.

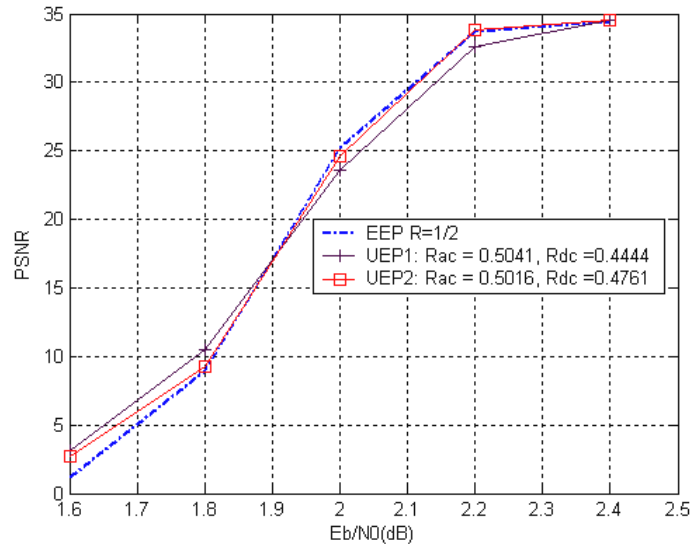
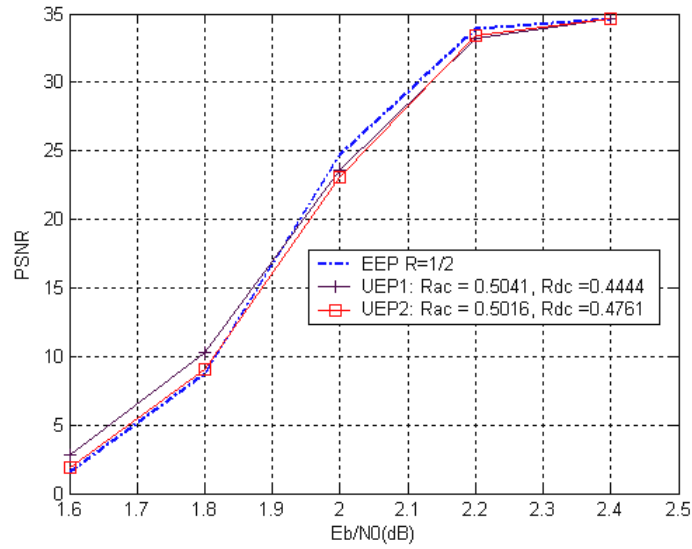
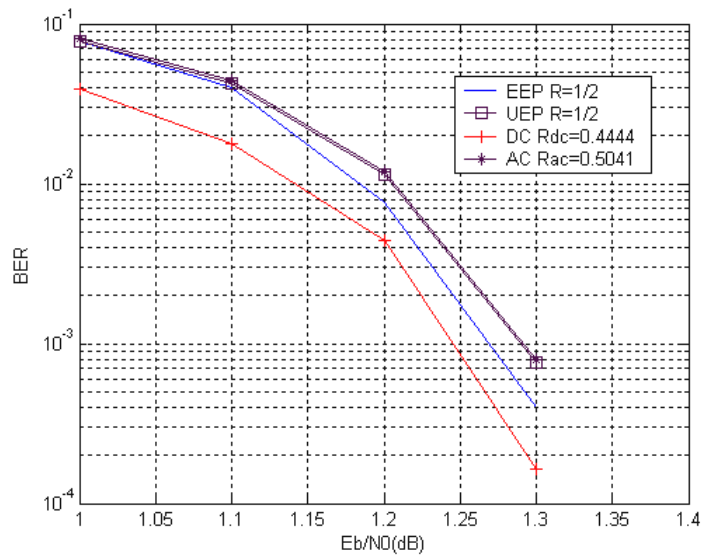


Fig. 5 – PSNR performance comparison of EEP and UEP scheme for  $S$ -random interleaver (1st structure type).



**Fig. 6** – PSNR performance comparison of EEP and UEP scheme for S-random odd-even interleaver (1st structure type).



**Fig. 7** – BER performance comparison of EEP and 1st UEP scheme for S-random interleaver (1st structure type).

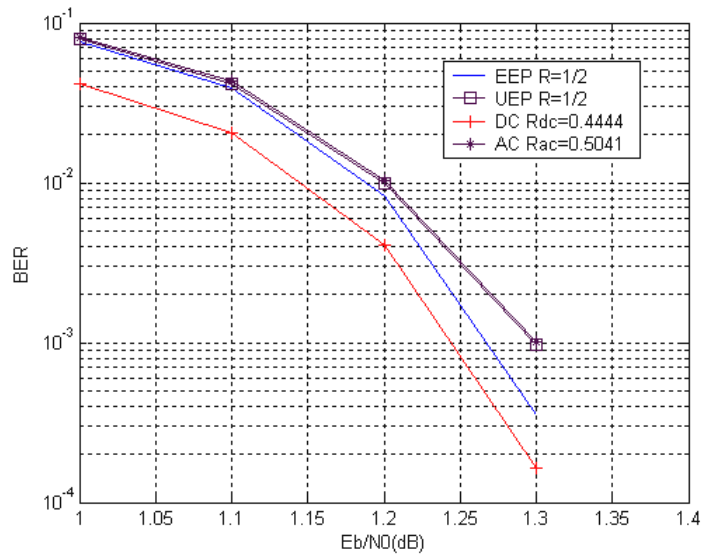


**Fig. 8** – BER performance comparison of EEP and 1st UEP scheme for S-random odd-even interleaver (1st structure type).

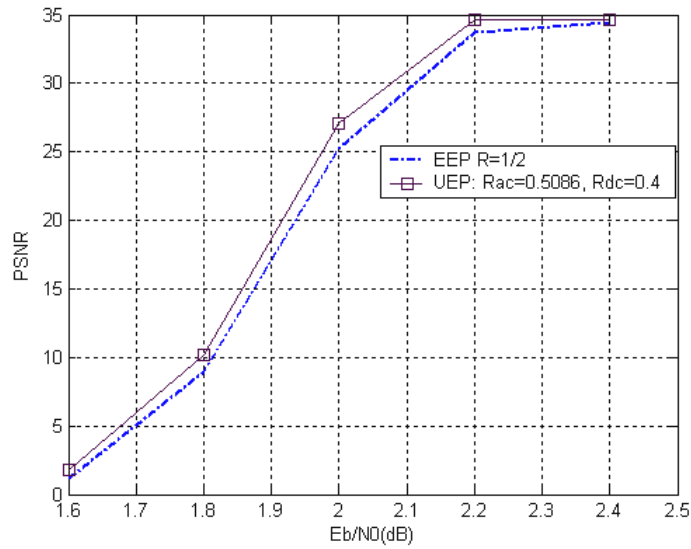


**Fig. 9** – PSNR performance comparison of EEP and UEP scheme for S-random interleaver (2nd structure type).

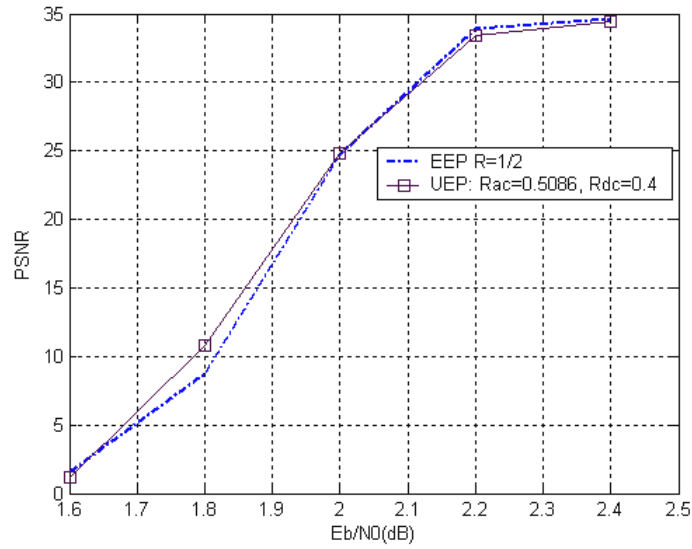


**Fig. 10** – PSNR performance comparison of EEP and UEP scheme for S-random odd-even interleaver (2nd structure type).

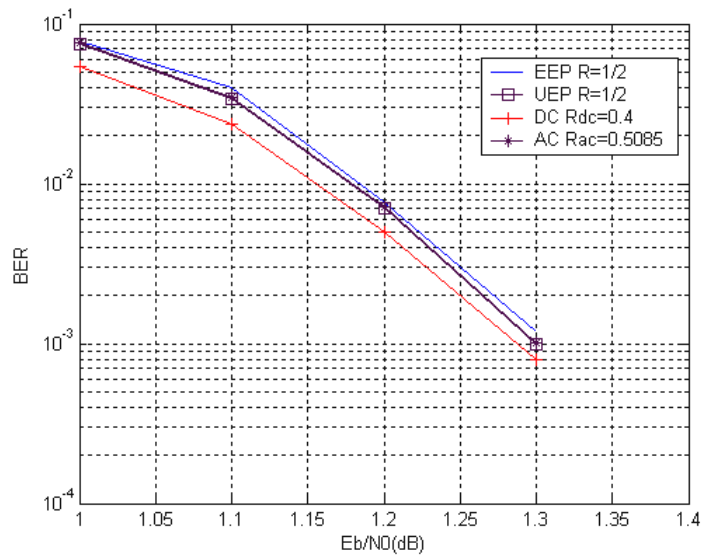


**Fig. 11** – BER performance comparison of EEP and UEP scheme for S-random interleaver (2nd structure type).

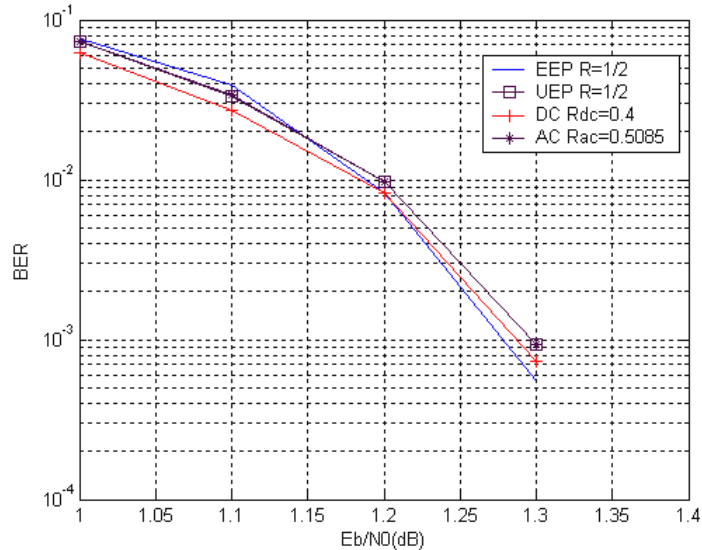


Fig. 12 – BER performance comparison of EEP and UEP scheme for S-random odd-even interleaver (2nd structure type).

## 5 Conclusion

UEP methods applied to JPEG image transmission using turbo codes are investigated in this paper. The DC and AC components are protected with different coding rates. Different UEP schemes are compared to that of EEP in terms of both BER and PSNR. The simulation results revealed:

1. The BER of highly sensitive DC bits is very sensitive to channel coding rate allocation. For S-random interleaver in second structure: A lower coding rate for DC components will lead to significant DC BER drop while keeping the corresponding AC BER inferior to that of EEP.
2. For very noisy channels, where  $E_b/N_0$  is relatively low, UEP schemes are better than EEP in terms of BER and PSNR. The average BER of the most important DC component is lower than that of EEP and UEP. For high  $E_b/N_0$ , the average PSNR of UEP schemes is worse than that of EEP except for S-random interleaver in second structure which is better. In this case the average BER of the AC component is lower than that of EEP.

## 6 References

- [1] ISO/IEC JTC1: Digital Compression and Coding of Continuous Still Images Part 1: Requirements and Guidelines, JPEG-9-R6 CD10918-1, 1991.

*A. Moulay Lakhdar, R. Méliani, M. Kandouci*

- [2] C. Berrou, A. Glavieux, and P. Thitimajashima: Near Shannon Limit Error-correction Coding: Turbo Codes, Proc. 1993 IEEE International Conference on Communications, Geneva, Switzerland, pp. 1064-1070, May 1993.
- [3] X. Fei and T. KO: Turbo-codes sed for Compressed Image Transmission Over Frequency Selective Fading Channel, IEEE GZobecom'97, New York, NY, USA, Vol. 2, pp. 629-633, Nov. 1997.
- [4] S. Le Goff: Les Turbo-codes et Leurs Applications Aux Transmissions à Forte Efficacité Spectrale, Thèse de doctorat de l'Université de Bretagne Occidentale, Brest, Nov. 1995.
- [5] J. Briffa: Interleavers for Turbo Codes, Master of Philosophy of the University of Malta, October 1999.
- [6] Small World Communications: Iterative Decoding of Parallel Concatenated Convolutional Codes, Application Note, 13 January 1999 (Version 1.4).
- [7] W. Xiang, S.A. Barbulescu, and S.S. Pietrobon: Unequal Error Protection Applied to JPEG Image Transmission using Turbo Codes, in Proc. IEEE Inform. Theory Workshop (ITW'01), Cairns, Australia, Sept. 2001, pp. 64-66.
- [8] J. Hagenauer: Rate-compatible Punctured Convolutional Codes (RCPC codes) and their Applications, IEEE Trans. Commun., Vol. 36, No. 4, pp. 389-400, Apr. 1989.
- [9] Z. Zhou, C. Xu: An Improved Unequal Error Protection Turbo Codes, IEEE Conference in Signal Processing., Vol. 1, pp. 1890-1901, Nov. 2005.